MODELING OF GALILEO/NIMS EUROPA SPECTRA OF THE ANTI-JOVIAN AND TRAILING SIDES USING TWO ENDMEMBERS AND WATER ICE. G. B. Hansen, Department of Earth and Space Sciences, University of Washington, Box 351310, Seattle, WA 98195-1310 (ghansen@ess.washington.edu)

Introduction: The Near Infrared Mapping Spectrometer (NIMS) observations at wavelengths 0.7-5.3 μm of the Jovian moon Europa are being reprocessed using information gained throughout and beyond the Galileo mission. Early analysis of these reprocessed data (three observations, including a global scale one of the anti-Jovian and trailing hemispheres at 47 km spatial resolution) show evidence of spectral features not or only weakly apparent before [1]. These include strong absorption bands attributed to CO_2 and SO_2 (centered near 4.25 and 4.0 μm, respectively). The strong hydrate bands, including at near 1.5 and 1.95 μm, are now more clearly defined. The largest amounts of CO_2 and the most well defined hydrate bands are strongly associated with the (endogenic) dark reddish regions on the surface [1, 2]. We are now doing end-to-end spectral modeling of the newly calibrated observations.

Europa is the second outward from Jupiter of the four Galilean satellites. It is similar in size to the Earth's moon, and has a young crater-free surface. The interior has a dense rocky/metallic core surrounded by a low density shell 80-170 km thick that is assumed to be primarily ice and/or water. The magnetic signature of Europa implies the presence of a conducting liquid subsurface ocean. Additionally, spectra from Galileo/NIMS showed the surface to be partly covered by heavily hydrated materials such as sulfate salts [3, 4] and/or sulfuric acid hydrate [5, 6]. The hydrated material is concentrated in the regions of darker brownish coloring that occur in some chaos regions and along linea, and may be linked to possible endogenic materials from the subsurface [3].

Instrument: The NIMS builds up spectral images by recording a spectrum over 20 mirror positions and up to 408 wavelengths. These wavelengths are sensed by 17 discrete detectors, each of which covers a small region of the spectrum. The third dimension of the spectral image is filled out by scanning the instrument field-of-view slowly perpendicular to the mirror motion [7]. The NIMS observations of the icy satellites are now being reexamined and recalibrated using new techniques [8, 9, 10]. The Europa observations needed an improved despiking process for the spectra longer than 3 μm, where radiation spikes outnumber the good data by a ratio of 2:1, or more. The first Europa observation to be processed was TERINC (Terra Incognito) from the E6 orbit, which was known to have fewer spikes overall than average. This is a global scale observation with a pixel scale of 47 km

Calibration: Every observation is dark-corrected and radiometrically calibrated using the best dark and calibration values and wavelength list [11]. The wavelengths up to 2.4 μm were despiked using our usual procedure [12]. The short wavelengths have fewer than 50% spikes and are amenable to this process. For the wavelengths longer than about 2.75 μm various despiking strategies are used, from the usual procedure, tightened and repeated (used on TERINC), to constraining to an envelope around the observation average spectra (used on all other observations to date). The wavelengths beyond 4.4 μm have just a few digital numbers (DN) of signal, and contain no information other than a general shape. The frequency of spikes in this region was 70-80% in TERINC and greater than 90% on all other observations. Two additional Europa data sets were calibrated in 2007, SUCOMP2 (pixel scale 7.5 km) [2] from orbit 6 and LINEA (pixel scale 17 km) from orbit 3.

Observation and Modeling: We finished a new observation early this year, which we used to develop the spectral model and get it working. The results for the G1NHILAT cube, a global view from the first orbit with a pixel scale of 79 km were presented in [13]. The calibration and projection were complicated by the fact that the two parts of the cube were recorded in different gain states and projected separately in the PDS data. In addition, this cube was "recovered" from garbled data caused by computer upsets that lost some of the original data. This results in a projected cube with many artifacts that had to be corrected.

We have now applied the spectral model to the TERINC observation, which covers much of the NHILAT observation at higher spatial resolution. We performed linear modeling of this observation along the lines of [14], using two hydrates and water ice of various grain sizes. The first hydrate was taken from the data, equivalent to the "average" hydrate spectrum from [3] (Figure 3). In addition we used a wavelength-extended version of sulfuric acid hydrate from [5, 6] (Figure 3). A scaling function taken to a variable power is used to modify the first hydrate spectrum to account for photometric variation (Figure 4). A bidirectional reflectance model for water ice (at a temperature of 110 K) with 10 grain sizes was created for the lighting geometry of the cube as a third component. The water

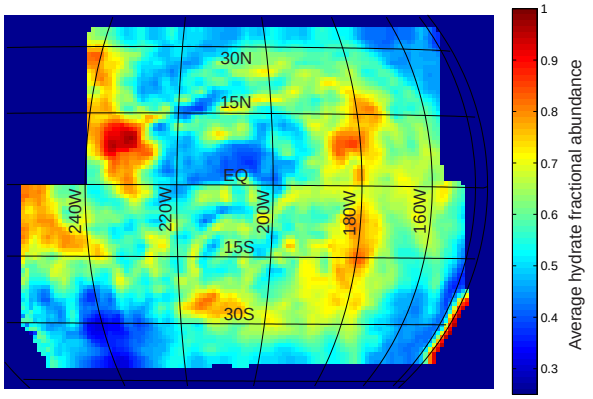

Figure 1. Average hydrate fractional abundance.

ice models are interpolated to create intermediate grain sizes.

Results: In general the fits are better than in [14], partly because of the use of continuous rather than discrete ice grain sizes. The model allows for two distinct grain sizes (bimodal), but this is used in this observation only in the upper right corner. Figure 1 shows the average hydrate abundance, Figure 2 shows the abundance of sulfuric acid hydrate and Figure 3 shows the water ice abundance. These values are normalized to one given the water ice abundance as quantitative.

The average hydrate is concentrated in the dark linea and chaos regions. The ice is most abundant in the polar regions, although there is 30-40% in some equatorial regions. The acid hydrate is constrained to the trailing side and low latitudes coincident with the particle radiation that creates it. It is also modified by water abundance, since it requires water ice for the reaction.

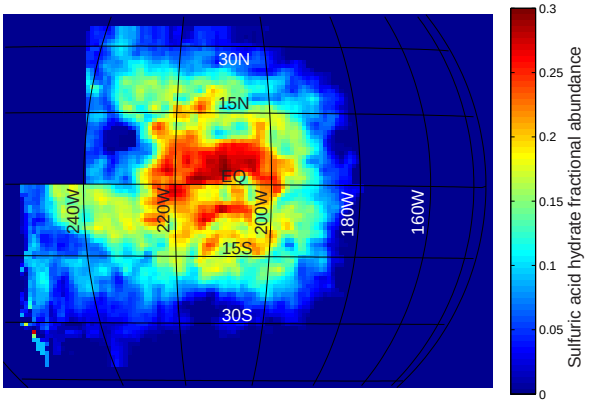

Figure 2. Sulfuric acid hydrate fractional abundance.

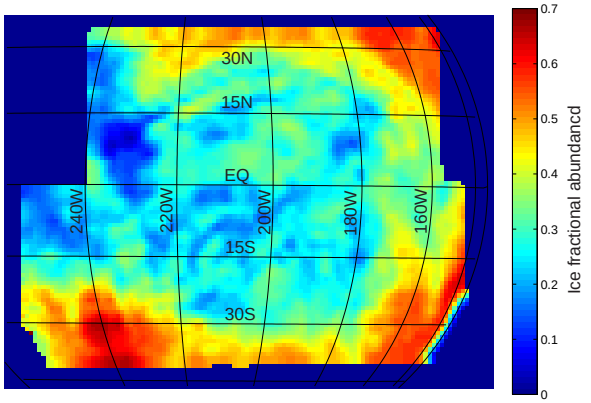

Figure 3. Water ice fractional abundance.

Discussion and Future Work: The model makes good fits with only two endmembers and water ice. The results from TERINC are also more or less consistent with the earlier results from NHILAT. The distribution of acid hydrate is more or less as expected. I plan to model the two remaining calibrated cubes and also the two other cubes in orbit C3 next.

References: [1] Hansen, G. B., and McCord, T. B. (2008) *GRL, 35*, L01202. [2] McCord, T. B., et al. (2010) *Icarus, 209*, 639-650. [3] McCord, T. B., et al. (1999) *JGR, 104*, 11,827-11,852. [4] McCord, T. B., et al. (2002) *JGR, 107(E1)*, 5004. [5] Carlson, R. W., Johnson, R. E., and Anderson, M. S. (1999) *Science, 286*, 97-99. [6] Carlson, R. W., et al. (2005) *Icarus, 177*, 461-471. [7] Carlson R. W.,et al. (1992) *Space Sci. Rev., 60*, 457-502. [8] Hansen, G. B., and McCord, T. B. (2004) *JGR, 109*, E01012. [9] Hansen, G. B., et al. (2006) *BAAS., 38*, 540. [10] Hansen, G. B., and McCord, T. B. (2008) *BAAS, 40*, 506-507. [11] McCord, T. B., et al. (1999) *JGR, 104*, 27,157-27,162. [12] Hibbitts, C. A., McCord, T. B., and Hansen, G. B. (2000) *JGR, 105*, 22,541-22,557. [13] Hansen, G. B. (2011) EGSC-DPS2011, Abstract #589. [14] Shirley, J. H., et al. (2010) *Icarus, 210*, 358-384.